Determination of Magnetostrictive Stresses in Magnetic Rare-Earth Superlattices by a Cantilever Method

M. Ciria,[1] J. I. Arnaudas,[1] A. del Moral,[1] G. J. Tomka,[2] C. de la Fuente,[1] P. A. J. de Groot,[2] M. R. Wells,[3] and R. C. C. Ward[3]

[1]*Unidad de Magnetismo de Sólidos, Departamento de Física de la Materia Condensada and Instituto de Ciencia de Materiales de Aragón, Universidad de Zaragoza and Consejo Superior de Investigaciones Científicas, 50009, Zaragoza, Spain*

[2]*Physics Department, University of Southampton, Southampton SO9 5NH, United Kingdom*

[3]*Oxford Physics, 5 Clarendon Laboratory, Parks Road, Oxford, OXI 3PU, United Kingdom*

(Received 20 January 1995)

The magnetostrictive stress for a Ho_6/Y_6 superlattice has been determined at low temperatures by means of a capacitive cantilever technique. The magnetostrictive stress responsible for the basal plane distortion is found to be strongly enhanced with respect to bulk holmium. An explanation accounting for the unusual thermal dependence of that stress is offered.

PACS numbers: 75.50.Rr, 75.80.+q

Magnetic rare-earth superlattices are a subject of great current interest [1–7]. Two features are remarkable in these artificial structures. First of all, helical magnetic order is found to propagate through nonmagnetic layers. This effect has been explained within the framework of the RKKY interaction through a spin density wave and the discreteness of the interleaving material which produces an increase of the magnetic period (aliasing effect) [8]. Also, discretness in the spin distribution increases the range of the interaction [8]. Second, different magnetic phases are identified in the superlattices when comparison with bulk is made. The strain induced in the crystalline structure by the mismatch between layers of different elements is thought to be responsible for such new magnetic behavior. The strain can couple to the magnetization either by modifying the indirect exchange, as was suggested to explain the suppression of the conical c-axis ferromagnetic transition in Er/Y [2], or by altering the energy balance between the exchange and magnetoelastic contributions. The latter mechanism accounts for the suppression of the ferrohelix first order transition in Dy/Y [3], where the Dy lattice is expanded, and for the enhancement of the Curie temperature in Dy/Lu [4], where Dy lattice is compressed. Similarly, while in Ho/Y the c-axis cone phase is suppressed and the critical fields are larger than in bulk [5,6], in Ho/Lu ferromagnetic order is observed below 30 K within Ho blocks containing less than 20 atomic planes [6,7]. Thus the knowledge of the magnetoelastic properties, which could provide the key to the epitaxial strain role in the magnetic behavior, is essential for a complete understanding of the magnetism of such new artificial materials. To date, magnetoelastic measurements in thin films and multilayers have been performed on polycrystalline or amorphous samples either directly, by means of the cantilever technique (*at room temperature* [9] and *in situ* at the growing chamber [10]) or indirectly, by studying the effect of stress in some magnetic properties (e.g., anisotropy field [11] and strain modulated ferromagnetic resonance [12]). In this paper we report on the first direct measurements of magnetostrictive stresses on magnetic superlattices by using a capacitive cantilever technique.

A $[Ho_6/Y_6]_{100}$ superlattice was grown by molecular beam epitaxy using a Balzers UMS 630 facility. The rare-earth metals grow epitaxially onto a Nb metal layer deposited on a sapphire substrate [5]. Both the body-centered-cubic Nb and hexagonal-close-packed rare-earth (RE) metals grow with their respective close-packed atomic planes parallel to the substrate plane. The epitaxial relationships are $\{11\bar{2}0\}Al_2O_3\|\{110\}Nb\|\{0001\}RE$, resulting in the a axis of the rare earth at an angle of 5° with [0001] Al_2O_3. The crystalline structure of the superlattice was investigated using a triple-crystal x-ray diffractometer, giving an interface width of ± 2 lattice planes [5]. The sapphire substrate, with initial thickness of 500 μm, was thinned down to 150 μm to increase the sensitivity of the cantilever method. The metallic superlattice acts as the central electrode of a three terminal differential capacitance cell. The cell was made in copper and annealed at 800 K to improve its behavior under thermal cycling. The capacitance measurements have been performed by using a AΣL Ltd. commercial ratio bridge, with phase sensitive detection. The sensitivity is 10^{-6} pF, which allows us to detect deflections of $\approx$10 nm for a sample length of 10 mm.

We will analyze the magnetoelastic measurements described below in terms of the deformation of the magnetic superlattice, as has been done when the cantilever method is employed. However, the existing relationships [13] linking magnetostriction, magnetoelastic stress, and deformation of the cantilever plate are only valid for polycrystalline films deposited onto isotropic substrates. For our derivation of expressions adequate for anisotropic systems, such as sapphire (orthorhombic, class $\bar{3}m$), we apply the theory of pure bending of plates [14]. It is assumed that for thin plates the stress components

 0031-9007/95/75(8)/1634(4)$06.00 © 1995 The American Physical Society

σ_{iz} ($i = x, y, z$; the z direction being normal to the plate surface) are zero and the strains on the plane ϵ_{ij} ($i, j = x, y$) are proportional to the curvatures: $\epsilon_{xx} = z/R_x$ and $\epsilon_{yy} = z/R_y$, where $1/R_x$ and $1/R_y$ are the curvatures in the x-z and y-z planes. Then $\sigma_{xx} = (C_{xx}/R_x + C_{xy}/R_y)z$ and $\sigma_{yy} = (C_{yy}/R_y + C_{xy}/R_x)z$, where the C_{ij} stand for combinations of sapphire elastic constants related to a coordinate system in which x and y directions correspond to the b and a superlattice axes, respectively. Now, to obtain the relationship between curvatures and magnetoelastic strains we will minimize the energy of the system, i.e., sapphire substrate plus superlattice. The elastic energy of sapphire is

$$E_{\mathrm{sa}} = \frac{1}{2}\left(\frac{C_{xx}}{R_x^2} + \frac{2C_{xy}}{R_yR_x} + \frac{C_{yy}}{R_y^2}\right)ah_{\mathrm{sa}}^3\left(\beta^2 - \beta + \frac{1}{3}\right), \tag{1}$$

where a and h_{sa} are the area and thickness of the sapphire substrate, and β is defined in such a way that βh_{sa} is the distance from the neutral surface to the superlattice surface. The elastic and magnetoelastic first order contributions to the energy density for the superlattice is $e_{\mathrm{sl}} = (1/2)c_{ijkl}\epsilon_{ij}\epsilon_{kl} - B_{ij}\epsilon_{ij}\alpha_i\alpha_j$, where c_{ijkl} are the elastic stiffness constants, α_i the direction cosines of the magnetization, and B_{ij} magnetoelastic coefficients. Notice that e_{sl} must be invariant under the symmetry operations of the D_{3h} group corresponding to the hexagonal-close-packed structure. Since the superlattice thickness h_{sl} is negligible compared to the sapphire one, we have assumed that the deformation is uniform in the superlattice. Taking $z = \beta h_{\mathrm{sa}}$ in the strain expressions, we obtain for the superlattice $\epsilon_{xx} = \beta h_{\mathrm{sa}}/R_x$ and $\epsilon_{yy} = \beta h_{\mathrm{sa}}/R_y$. When the magnetization is along the easy direction, we obtain ϵ_{zz} in the superlattice by minimizing e_{sl}, where the above values for ϵ_{xx} and ϵ_{yy} are used. The total energy of the system is contributed by the magnetoelastic energy of the superlattice and by the elastic energy of the sapphire, the elastic contribution being negligible for the superlattice and then neglected. Now, minimizing the total energy with respect to β, $1/R_x$, and $1/R_y$ we get $\beta = 2/3$ and

$$\mathcal{B} + \frac{1}{4}B^{\gamma} = \frac{1}{6}\frac{h_{\mathrm{sa}}^2}{h_{\mathrm{sl}}}\left(\frac{C_{xx}}{R_x} + \frac{C_{xy}}{R_y}\right), \tag{2a}$$

$$\mathcal{B} - \frac{1}{4}B^{\gamma} = \frac{1}{6}\frac{h_{sa}^2}{h_{sl}}\left(\frac{C_{yy}}{R_y} + \frac{C_{xy}}{R_x}\right), \tag{2b}$$

where $\mathcal{B}$ is a combination of α-magnetoelastic and elastic constants of the superlattice. From Eq. (2) we obtain the value of the magnetoelastic coupling parameter B^{γ} by experimentally determining $1/R_x$ and $1/R_y$. It is worth noting that by using the present technique B^{γ} is directly obtained and no knowledge of the elastic constants of the superlattice is needed. This is important if one considers the difficulty of determining such constants and that bulk elastic constants are not applicable to superlattices [15]. Equations (2) hold for a free superlattice. In our case the sample is clamped by one of its edges. This condition imposes that the clamped edge does not undergo vertical displacement and remains horizontal in the deformation. Therefore we can assume that the curvature of the plate is produced in the plane perpendicular to the clamping line. So that for the sample clamped along a direction we use Eq. (2a) putting $1/R_y = 0$, and we relate $\tilde{\sigma}_a \equiv \mathcal{B} + B^{\gamma}/4$ with $1/R_x$. Conversely, Eq. (2b) with $1/R_x = 0$ is used for clamping along the b direction, and we obtain another relation between $\tilde{\sigma}_b \equiv \mathcal{B} - B^{\gamma}/4$ and $1/R_y$. The curvatures are determined by measuring the respective capacitance changes and using the expression $\Delta C = -C_0^2L^2/6\varepsilon_0AR$, valid for small deflections, where C_0 is the zero-field capacity, ε_0 is the permitivity of vacuum, and L, A, and $1/R$ are the length, area, and curvature of the plate. Thus the expression of B^{γ} is obtained in terms of the different experimental values for both kind of measurements, i.e., a sample clamped along a and b directions, in the form

$$B^{\gamma} = -\frac{2\varepsilon_0h_{\mathrm{sa}}^2}{h_{\mathrm{sl}}}\left(C_{xx}\frac{A_a\Delta C_a}{L_a^2C_{0a}^2} - C_{yy}\frac{A_b\Delta C_b}{L_b^2C_{0b}^2}\right), \tag{3}$$

where C_{xx} and C_{yy} are calculated from Ref. [16].

It is worth mentioning that the differential thermal expansion of superlattice and sapphire induces an initial curvature so that the C_0 value is altered with respect to the ideal value considered for parallel capacitor plates. Nevertheless, it is easy to show that this effect on the B^{γ} parameter is negligible because it is obtained as the difference of two values which are modified in the same way by the differential thermal expansion. Both values are modified almost equally because the thermal expansion coefficient for the basal plane of the superlattice is isotropic and $h_{\mathrm{sa}} \gg h_{\mathrm{sl}}$. Also the dielectric constant of sapphire does not appear in Eq. (3) because the deflection is small.

Low temperature magnetoelastic stress measurements were performed in the $[\mathrm{Ho}_6/\mathrm{Y}_6]_{100}$ superlattice between 10 and 140 K. The magnetic field, produced by a 12 Tesla superconducting coil, was applied along the easy b direction. Each isotherm was obtained after annealing at temperatures within the paramagnetic state. In Fig. 1 we show the magnetoelastic stress isotherms obtained with the sample clamped along the a and b axes.

In bulk Ho, below the Néel temperature, $T_N = 133$ K, the moments are ferromagnetically confined to the basal plane forming an helical structure with the magnetic modulation wave vector along the c axis, which is reduced on cooling. Below the Curie temperature, $T_C = 20$ K, the moments tilt out of the basal plane to form a cone structure [17]. In bulk holmium and other rare-earth metals the breakdown of the helical spin state to reach a structure of spins parallel to the field is accompanied by a large increase in the strain [18]. We find the same effect in the superlattice (see Fig. 1). At low temperatures the

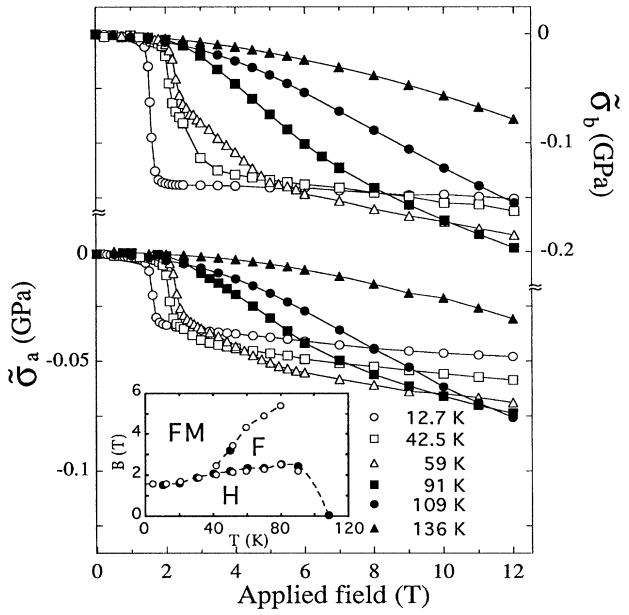

FIG. 1. Magnetoelastic stress isotherms: $\tilde{\sigma}_a$ and $\tilde{\sigma}_b$ correspond to clamping along a and b superlattice axes. Inset shows the magnetic phase diagram obtained from magnetostriction (○) and magnetization (●) measurements (B are the phase transition fields).

sudden onset of the stress and saturation, at a critical field B_c, is interpreted as a direct transition to a ferromagnetic state. As the temperature is raised, we observe that the strain increases less abruptly, although changes in the slope can be detected. We interpret these changes in terms of the field distortion of the helix producing a fan structure at B_{c1}, and a ferromagnetic nonsaturated state is reached above a field B_{c2}. For the present sample, T_N values of 95 and 108 K have been determined from neutron diffraction [5] and magnetization [6] experiments, respectively. The isotherms at temperatures close to T_N depart from the expected B^2 paramagnetic behavior for fields above $\approx$5 T, likely as a consequence of short-range magnetic order, the quadratic field dependence up to 12 T being reached at temperatures above $\approx$135 K. The phase diagram determined from the anomalies of the gradient of the magnetoelastic stress curves is shown in the inset of Fig. 1. We have also included the points identified by magnetization measurements [6], which closely agree with that determined by magnetoelastic stress measurements. The fields below which the zero field structure exists are much larger than in bulk Ho, while the temperature dependence is weaker. The fan structure appears above 40 K and remains stable in progressively larger fields as the temperature is raised.

In Fig. 2 we plot the thermal variation of B^γ at the maximum applied field of 12 T and the one for bulk holmium [19], $B^\gamma_{\rm bulk}(T)$, for comparison, normalized to the corresponding Ho volume in the superlattice.

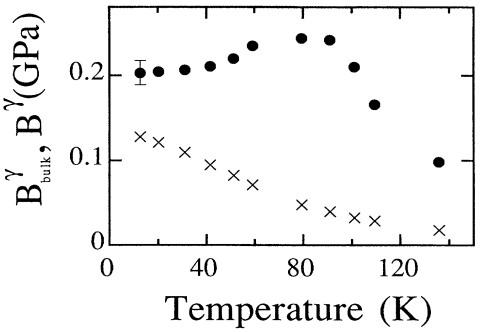

FIG. 2. Thermal variation of the effective magnetoelastic coupling parameter B^γ for the $[Ho_6/Y_6]100$ superlattice (•). For comparison, $B^\gamma_{\rm bulk} = B^\gamma_{\rm bulk}(0)\hat{I}_{5/2}[\mathcal{L}^{-1}(m(T))]$ is shown (×).

The B^γ values are enhanced with respect to those for bulk Ho. Unlike the bulk case, the thermal variation of B^γ does not follow the $\hat{I}_{5/2}[\tilde{m}] \equiv \hat{I}_{5/2}[\mathcal{L}^{-1}(m(T))]$ standard Callen and Callen law [20] at all [$m(T) \equiv M(T)/M(0)$ is the reduced magnetization]. To explain these results we will show how the epitaxial strain affects the magnetoelastic coefficient. An enhancement of this coefficient has been also observed in isotropic multilayers [12] and surfaces [21] under tensile stress. This is consistent with our case, in which thin Ho films are decoupled by interleaving films of Y.

Sun and O'Handley [21] argued that the presence of strains of $\sim$1% modifies the magnetoelastic coefficients. So, we assume that their effective form, expanding in the strains is:

$$B_{ij}(T) = M_{ij}(T) + D_{ijkl}(T)\epsilon_{kl}\,, \qquad (4)$$

where $M_{ij} = (B_{ij})_{\epsilon_{kl}=0}$ and $D_{ijkl} = (\partial B_{ij}/\partial\epsilon_{kl})_{\epsilon_{kl}=0}$. These may involve both surface and volume contributions. Thus the thermal dependence of B_{ij} arises from that of the magnetoelastic coefficients M_{ij} and D_{ijkl}, as well as from the variation with temperature of the epitaxial strain due to the lattice misfit between Ho and Y layers. As well as the strain linear term, the strain quadratic term in the magnetoelastic Hamiltonian is written as a product of isomorphous irreducible representations of the same second order spin operators times second order strain polynomials [22], and then we will have the same $\hat{I}_{5/2}[\tilde{m}]$ thermal variation for M_{ij} as for D_{ijkl}. The mismatch between bulk Ho and Y, ϵ_b, at room temperature is $\sim$2%, the basal plane of Ho being stretched with respect to the bulk. The total strain ϵ_{ii} is contributed to by the epitaxial strain ϵ^{ep}_{ii} and the magnetoelastic strain ϵ^{me}_{ii}. On the basal plane $\epsilon^{ep}_{xx} = \epsilon^{ep}_{yy} = \epsilon_0$ and ϵ^{ep}_{zz} is deduced from the strain-stress relations taking $\sigma_{zz} = 0$. Also $\epsilon_0 \gg \epsilon^{me}_{ii}$ is assumed. Then, we can write

$$B^\gamma(T) = [M^\gamma(0) + D(0)\epsilon_0(T)]\hat{I}_{5/2}[\tilde{m}(T)]\,. \qquad (5)$$

We will show that the peculiar thermal dependence of B^γ below $\simeq$100 K is due to that of ϵ_0, which below

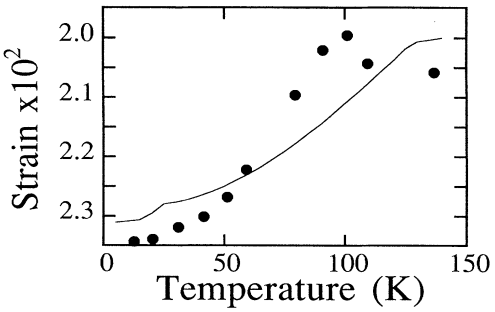

FIG. 3. Temperature dependence of the bulk Ho and Y mismatch strain, ϵ_b (line), calculated from the respective a lattice parameters thermal expansion data [19,23]. Also shown is the epitaxial strain, ϵ_0, thermal variation (•).

T_N is mainly contributed by the magnetic thermal expansion of Ho layers. In Fig. 3 we represent $\epsilon_0(T)$ as obtained from the experimental B^γ by using Eq. (5), with $M^\gamma(0) = 4.7$ GPa and $D(0) = -191$ GPa, together with $\epsilon_b(T)$ [19,23]. We observe that the obtained ϵ_0 thermal dependence strongly resembles that of ϵ_b, as should be expected [in fact, $\epsilon_0(300\ \mathrm{K}) \simeq 0.015$ [5] and $\epsilon_b(300\ \mathrm{K}) \simeq 0.020$]. Although $D(0)$ is 2 orders of magnitude larger than $M^\gamma(0)$, notice that the first is the strain *derivative* of the latter, and if the term $D(0)\epsilon_0(T)$ in Eq. (5) has to determine the low temperature dependence of B^γ, it has to be, at least, 2 orders of magnitude larger than $M^\gamma(0)$, considering that $\epsilon_0(T) \simeq 0.015$ at room temperature.

Summarizing, we have developed for the first time a cantilever technique working at liquid helium temperatures in order to determine magnetoelastic stresses in *anisotropic* magnetic superlattices. It is noticeable that the important magnetoelastic coupling parameter B^γ obtained for a $[Ho_6/Y_6]100$ superlattice is enhanced with the respect to the bulk Ho value up to 6 times.

We wish to thank F. Villuendas for technical help and acknowledge financial support by the Spanish CICYT, Grants No. PB91-0936 and No. PB90-1014, the British SERC and the British Council and Spanish Government Acc. Int. HB 94/B. One of us (M.C.) is grateful to Standard-Alcatel for a postgraduate research grant.

[1] C.F. Majkrzak, J. Kwo, M. Hong, Y. Yafet, Doon Gibbs, C.L. Chien, and J. Bhor, Adv. Phys. **40**, 99 (1991).
[2] J.A. Borchers, M.B. Salamon, R.W. Erwin, J.J. Rhyne, R.R. Du, and C.P. Flynn, Phys. Rev. B **34**, 3123 (1991).
[3] R.W. Erwin, J.J. Rhyne, M.B. Salamon, J.A. Borchers, Shantanu Sinha, R. Du, J.E. Cunningham, and C.P. Flynn, Phys. Rev. B **35**, 6808 (1987).
[4] R.S. Beach, J.A. Borchers, A. Matheny, R.W. Erwing, M.B. Salamon, B. Everitt, K. Pettit, J.J. Rhyne, and C.P. Flynn, Phys. Rev. Lett. **70**, 3502 (1993).
[5] D.A. Jehan, D.F. McMorrow, R.A. Cowley, R.C.C. Ward, M.R. Wells, N. Hagmann, and K.N. Clausen, Phys. Rev. B **48**, 5594 (1993).
[6] G.J. Tomka, P.A.J. de Groot, B.D. Rainford, M.R. Wells, R.C.C. Ward, J.I. Arnaudas, A. del Moral, and M. Ciria (to be published).
[7] P.P. Swaddling, D.F. McMorrow, J.A. Simpson, R.C.C. Ward, M.R. Wells, and K.N. Clausen, J. Phys. Condens. Matter **5**, L481 (1993).
[8] P. Bruno and C. Chappert, Phys. Rev. B **46**, 261 (1992), and references therein.
[9] E. Klokholm, IEEE Trans. Magn. **12**, 819 (1976); K. Twarowski and H.K. Lachowicz, Phys. Status Solidi (a) **53**, 599 (1979); H. Awano, Y. Suzuki, T. Yamazki, T. Katayama, and A. Itoh, IEEE Trans. Magn. **26**, 2742 (1990).
[10] M. Weber, R. Koch, and K.H. Reider, Phys. Rev. Lett. **73**, 1166 (1994).
[11] E.N. Mitchell and G.I. Lykken, J. Appl. Phys. **33**, 1170 (1962).
[12] R. Zuberek, H. Szymczak, R. Krishnan, and M. Tessier, J. Phys. **49**, C8-176 (1988).
[13] E. du Trémolet de Lacheisserie and J.C. Peuzin, J. Magn. Magn. Mater. **136**, 189 (1994).
[14] S. Timoshenko and S. Woinowsky-Krieger, *Theory of Plates and Shells* (MacGraw-Hill, New York, 1959), 2nd ed.
[15] J.R. Dutcher, S. Lee, J. Kim, G.I. Stegeman, and C.M. Falco, Phys. Rev. Lett. **65**, 1231 (1990).
[16] W.E. Tefft, J. Res. Natl. Bur. Stand. Sect. A **70**, 277 (1966).
[17] W.C. Koehler, J.W. Cable, M.K. Wilkinson, and F.O. Wollan, Phys. Rev. **151**, 414 (1966).
[18] S. Legvold, J. Alstad, and J.J. Rhyne, Phys. Rev. Lett. **10**, 509 (1963).
[19] J.J. Rhyne, S. Legvold, and J. Alstad, Phys. Rev. **154**, 266 (1967).
[20] E. Callen and H.B. Callen, Phys. Rev. **139**, A455 (1965).
[21] S.W. Sun and R.C. O'Handley, Phys. Rev. Lett. **66**, 2798 (1991); R.C. O'Handley and S.W. Sun, J. Magn. Magn. Mater. **104-107**, 1717 (1992).
[22] E. du Trémolet de Lacheisserie, *Magnetostriction: Theory and Applications of Magnetoelasticity* (CRC Press, Boca Raton, FL, 1993).
[23] R.W. Meyerhoff and J.F. Smith, J. Appl. Phys. **33**, 219 (1962).